A switch in kappa opioid receptor signaling from inhibitory to excitatory induced by stress in a subset of cortically-projecting dopamine neurons

Elyssa B. Margolis[1*]

[1]UCSF Weill Institute for Neurosciences, Neuroscience Graduate Program, Department of Neurology, University of California, San Francisco, CA, United States

*Corresponding Author

Email: Elyssa.Margolis@ucsf.edu

Abstract

The kappa opioid receptor (KOR) has shown potential as a therapeutic target for several neuropsychiatric disorders including major depressive disorder, pain, and substance use disorder. *In vivo* signaling of G protein coupled receptors like the KOR is generally thought to change in magnitude but not sign in such behavior states. Here we investigated KOR modulation of ventral tegmental area (VTA) neurons following an acute, behaviorally aversive manipulation. We found this experience switches KOR signaling from inhibitory to excitatory in a subset of VTA dopamine neurons. Brief corticotrophin releasing factor (CRF) exposure *ex vivo* rapidly induces a similar switch in KOR signaling, specifically in dorsal medial prefrontal cortex (dmPFC) projecting neurons, but not nucleus accumbens or basolateral amygdala projecting neurons. These KOR mediated excitations depend on G protein activation, but where somatodendritic VTA KORs activate a K^+ conductance to hyperpolarize dopamine neurons in control conditions, depolarizations require hyperpolarization-activated cyclic nucleotide-gated channel (HCN) function. One behavioral impact of this change is a loss of the aversiveness of intra-VTA KOR activation, providing direct evidence that rapid changes in signaling coupling of one GPCR can be triggered by activity at other GPCRs thus significantly altering behavioral responses driven by neuromodulators.

Introduction

Activation of the KOR system mediates immediate processing of and long-lasting behavioral changes in response to aversive stimuli. Pharmacological blockade or genetic inactivation of KORs can decrease the acute aversiveness of stressors, including pain, and promote resilience to the development of depressive-like behaviors including decreased food reward seeking, decreased social interactions, and increased immobility in forced swim and social defeat paradigms[1–4]. Therefore, KOR antagonism has been proposed as a therapeutic approach to neuropsychiatric disorders with symptom profiles that include aversive emotional and anhedonic states, such as anxiety and depression, and to mitigate stress induced relapse to drug use[5].

The opioid receptor family of GPCRs commonly signals via inhibitory Gαi/o activation[6]. Agonists at somatodendritic KORs hyperpolarize neurons in a variety of brain regions including the dorsal raphe, nucleus raphe magnus, and ventral pallidum[7–9]. In the VTA, KOR activation inhibits a subset of dopamine neurons through G protein-gated inwardly rectifying K^+ channel (GIRK) activation while non-dopamine neurons show no response[10]. Behaviorally, KOR activation in the VTA is aversive[11], and intra-VTA blockade of KORs prevents the aversiveness of systemic KOR agonist administration[12]. Intra-VTA KOR blockade also prevents stress induced reinstatement of cocaine seeking[13]. Paradoxically, aversive stress blunts some physiological KOR responses, such as the KOR coupled GIRK conductance in serotonergic dorsal raphe neurons[8]. Understanding KOR function in relevant behavior states will improve our ability to treat the target neuropsychiatric disorders.

Here we investigated postsynaptic KOR agonist responses in VTA neurons after an acute aversive stressor in order to improve our understanding of what functionality KOR antagonism might have in a therapeutically relevant state. Rather than a change in response magnitude, acute aversive stress caused a change in the sign of the physiological response to KOR activation in a subset of VTA neurons. Importantly, this change was specific to VTA dopamine neurons projecting to the dmPFC, a site where dopamine function contributes to executive function and reward processing[14–17].

Results

We performed *ex vivo* whole cell recordings in rat VTA neurons after a single session of aversive foot shock stress, making slices 30-60 min after the stressor. All statistics are described in Table 1. In addition to VTA neurons that responded to the KOR selective agonist U69,593 (1 μM) with a hyperpolarization or no change in membrane potential similar to prior observations in untreated animals[10,18,19], we unexpectedly observed depolarizations in a distinct subset of neurons from both male and female rats (Fig. 1a-d). This includes neurons confirmed as dopaminergic with immunocytochemistry (Fig. 1b, Extended Data Fig. 1a; recording locations in Extended Data Fig. 1b). Depolarizations were still observed 3 (4/18 neurons), but not 5 (0/7 neurons), days after the foot shock stress session (Fig 1d). Action potential (AP) threshold was more depolarized in neurons from foot shock stressed rats compared to shams, but the stressor did not alter other basal properties of VTA neurons including baseline input resistance (Ri), AP duration, AP peak, h current magnitude, or spontaneous firing rate (Extended Data Fig. 2). In the recordings from stressed animals, initial Ri was greater in neurons that subsequently showed a depolarization in response to U69,593 compared to neurons that subsequently showed a hyperpolarization (Extended Data Fig. 3). No other differences were detected in baseline physiological properties across VTA neurons grouped by their U69,593 responses (Extended Data Fig. 3). One possibility is that the aversive stressor decreases GIRK function in a subset of neurons, unmasking the observed depolarizing effect of U69,593. However, when we blocked GIRKs in slices from control, untreated animals with $BaCl_2$ (100 μM), the distribution of responses to U69,593 was clearly different from those from stressed animals with no depolarization > 0.8 mV (Fig. 1d,e). Dopamine D2 receptor activation hyperpolarizes a subset of VTA neurons through GIRK channel activation[20]. If acute, aversive stress decreases GIRK function in VTA neurons rather than change KOR signaling, we would expect to observe a shift in responses to the D2R agonist quinpirole (1 μM) as well. The means and distributions of quinpirole responses were not different between VTA neurons from sham and foot shocked rats (Fig. 1f).

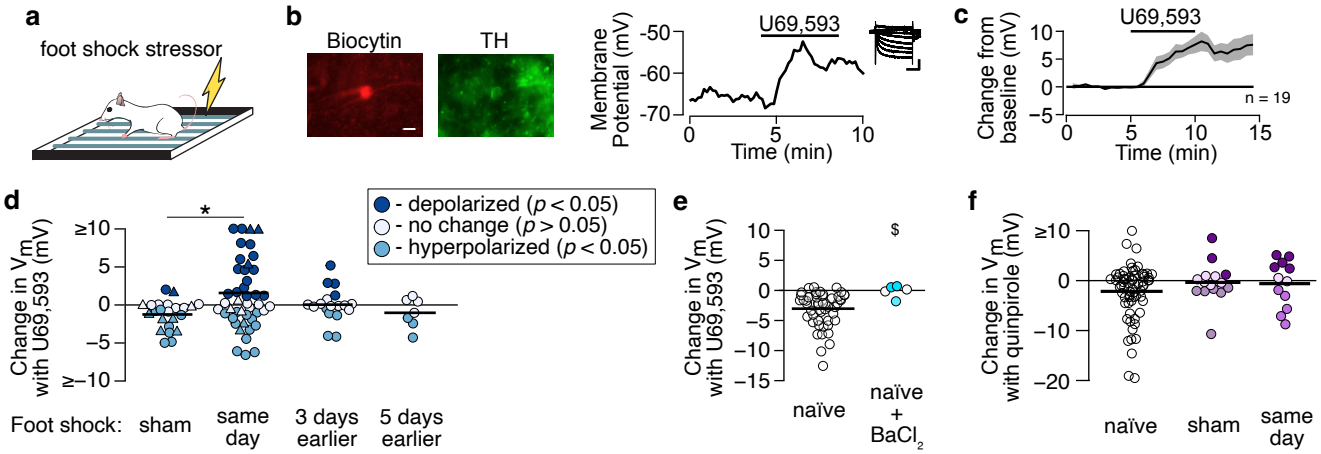

Figure 1. Following a single foot shock session, a subset of VTA neurons depolarize in response to KOR activation. *(a) Rats experienced a single intermittent foot shock session (10 min) prior to ex vivo whole cell recordings. (b) Example recording from a VTA neuron (biocytin fill: red) that was confirmed as dopaminergic with TH immunocytochemistry (green), scale bar 10 μm. In whole cell current clamp configuration (I = 0 pA) bath application of the KOR agonist U69,592 (1 μM) caused a depolarization. Inset: I_h measured in voltage clamp, scale bars 200 pA and 200 ms. (c) Mean time course of responses in neurons that were significantly depolarized*

by U69,593. (d) Summarized data, each circle is a neuron, from same day sham, same day shock, 3 days after shock, and 5 days after shock treated rats. Circles and triangles indicate VTA neurons from male and female rats, respectively. Permutation analysis comparing means of U69,593 responses in sham vs shock, p = 0.02 (Table 1) (e) Summarized U69,593 responses in VTA neurons from naïve rats, and from naïve rats where U69,593 responses were measured in $BaCl_2$ (100 μM). Permutation analysis comparing variances (SDs; $ indicates p<0.05), p = 0.04. (f) Summarized responses to the dopamine D2 receptor agonist quinpirole (1 μM) in VTA neurons from naïve, sham, and same day foot shocked rats. One way ANOVA sham vs shock, p = 0.9.

The corticotrophin releasing factor (CRF) system is upstream of the KOR system in encoding the aversiveness of stressful experiences[21], and blocking KORs can prevent CRF-induced anxiety-like behaviors[22,23]. As foot shock stress drives CRF release in the VTA[24], we tested the hypothesis that incubating VTA slices from control animals with no behavioral manipulations in CRF would produce similar changes in KOR signaling to the *in vivo* aversive stressor exposure. In fact, in VTA slices incubated in 200 nM CRF for 5 min, a subset of neurons responded to subsequent U69,593 application with a depolarization (Fig. 2a). Next we tested whether neurons excited by KOR activation after CRF were the same neurons inhibited by KOR activation under control conditions or a previously KOR-insensitive population. All neurons that showed a depolarization in response to KOR activation after CRF showed a hyperpolarization to KOR activation before CRF (Fig. 2b,c). In fact, for neurons that showed a depolarization after CRF, there was a clear inverse correlation (n = 5 neurons; coeff. = -0.9) between the magnitudes of KOR responses before and after CRF application (Fig. 2c).

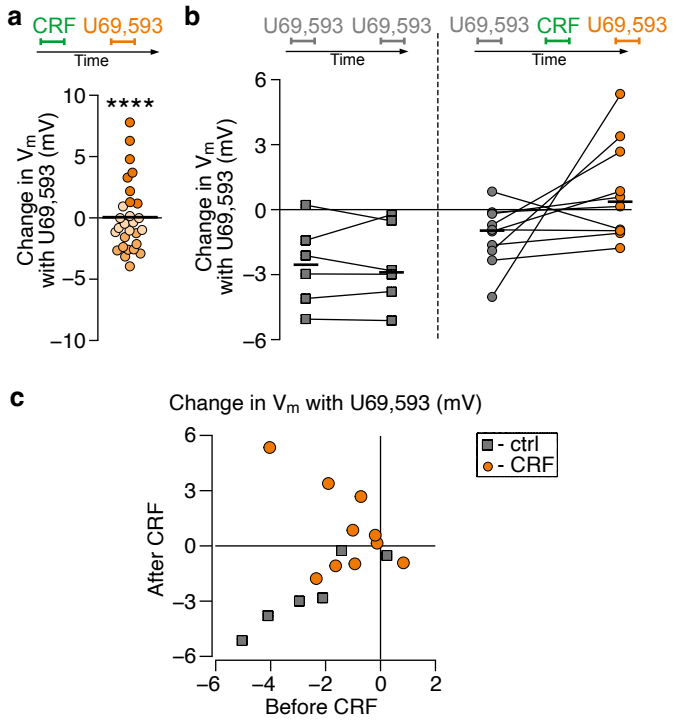

Figure 2. ex vivo exposure to CRF can switch KOR signaling from inhibitory to excitatory. *(a) Summarized data, each circle is a neuron. Slices were incubated for 5 min with CRF (200 nM), CRF was washed out for at least 5 min, then U69,593 (1 μM) was bath applied for 5 min. Statistical comparison to U69,593 responses in VTA neurons from naïve rats (Fig. 1e left), Permutation analysis of means, p = 0.00004. (b) Left, U69,593 (1 μM) was applied once, washed out, then reapplied (paired t-test p = 1.0). Right, U69,593 (1 μM) was applied once, washed out, CRF was washed on (5 min, 200 nM), washed out, then U69,593 was reapplied (paired t-test p = 0.08). (c) Data from (b) graphed as magnitude of response to first U69,593 application to second application.*

We previously reported that VTA dopamine neurons that project to the mPFC and basolateral amygdala (BLA), but not the nucleus accumbens (NAc), are inhibited by somatodendritic KOR activation in rat[18,19]. To test whether the signaling switch happens in a projection selective manner, we recorded from retrogradely labeled VTA neurons that project to dmPFC (including prelimbic and anterior cingulate cortices), ventral mPFC (infralimbic cortex), medial NAc, and BLA blind to injection site. Most distinctly, dmPFC-projecting VTA neurons showed the strongest depolarizations after CRF exposure while none of the vmPFC-projecting neurons depolarized (Fig. 3). NAc- and BLA-projecting showed no and minimal depolarizations, respectively (Fig. 3). Thus, the switch in KOR signaling from inhibitory to excitatory occurs in a specific subpopulation of dmPFC-projecting VTA neurons.

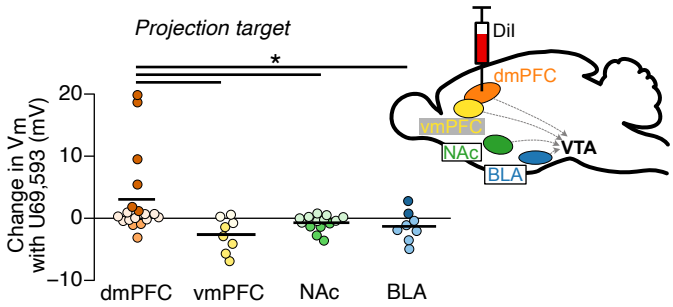

Figure 3. CRF switches KOR signaling in a subpopulation of dmPFC-projecting VTA neurons. *U69,593 responses were recorded in retrogradely labeled neurons after slices were incubated in CRF (5 min, 200 nM). Kruskal-Wallis rank sum test p = 0.006, pairwise comparisons listed in Table 1.*

Next we probed the signaling mechanism underlying the KOR mediated excitations triggered by CRF exposure. To test whether the KOR excitations are due to indirect effects involving local connectivity in the slice we measured KOR agonist responses while blocking AMPARs (10 μM DNQX), $GABA_A$Rs (20 μM gabazine), and action potential activity (500 nM TTX). This did not prevent U69,593 induced depolarizations (Fig. 4a). To block G protein signaling in the recorded neuron we included GDP-β-s in the intracellular solution (500 μM), and broke in to whole cell configuration only after CRF application was completed. This G protein block eliminated both depolarizations and hyperpolarizations induced by U69,593 (Fig. 4a). Together these data show that the KOR induced depolarizations are not local circuit dependent, and because the G protein blockade was limited to the recorded neuron the KORs in question appear to be expressed in the recorded neuron. GPCR activation could cause depolarization by closing GIRKs[25], however blocking GIRKs with $BaCl_2$ (100 μM) did not prevent U69,593 induced depolarizations (Fig. 4a). We previously reported that mu and delta opioid receptors (MORs and DORs) on VTA neurons can drive depolarizations that require Ca^{2+} channel conductances[26,27], however in the present study, blocking Ca^{2+} channels with bath application of $CdCl_2$ (100 μM) did not prevent U69,593 induced depolarizations (Fig. 4a). A Na^+ leak current contributes to the maintenance of a depolarized potential and spontaneous AP firing in VTA neurons[28,29] that can be inhibited by Gαi/o protein coupled receptors[30]. Blocking this conductance did not prevent U69,593 induced depolarizations (Fig. 4a).

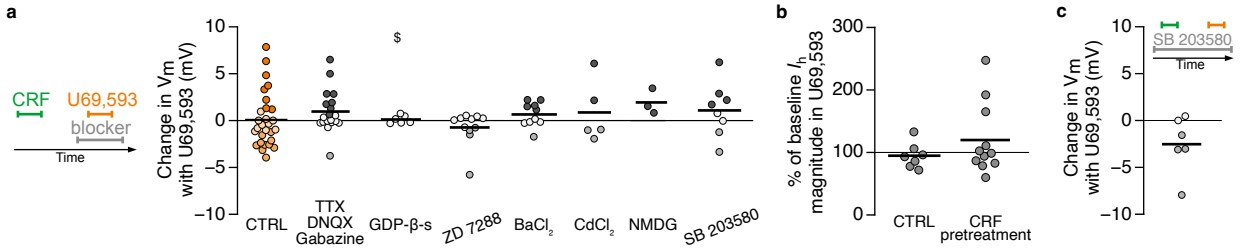

134

135 ***Figure 4. KOR mediated depolarizations require I_h.*** *(a) Signaling mechanism(s) that*
136 *contribute to U69,593 (1 μM) induced depolarizations were investigated after exposing slices ex*
137 *vivo to CRF (5 min, 200 nM). TTX (500 nM), DNQX (10 μM), and gabazine (20 μM) blocked*
138 *synaptic transmission; intracellular GDP-β-s (500 μM) blocked intracellular G protein signaling;*
139 *ZD7288 (10 μM) blocked HCN channels (I_h); $BaCl_2$ (100 μM) blocked K^+ channels; $CdCl_2$ (100*
140 *μM) blocked Ca^{2+} channels; replacement of Na^+ with NMDG (151 mM, replacing NaCl) in aCSF*
141 *blocked Na^+ leak current; SB203580 (10 μM) blocked p38/MAPK signaling. (b) I_h magnitude*
142 *was measured during U69,593 (1 μM) application in voltage clamp, stepping from -60 mV to -*
143 *120 mV, in control slices or slices pretreated with CRF (5 min, 200 nM). (c) p38/MAPK was*
144 *blocked with SB203580 application during both CRF and U69,593 application.*

145

146 I_h is a hyperpolarization activated, non-selective cation conductance that we found is prominent
147 in mPFC-projecting VTA neurons[19]. In nodose ganglion neurons MOR activation inhibits I_h[31],
148 and in the nucleus raphe magnus (NRM) KOR activation augments I_h[32]. The I_h blocker ZD7288
149 prevented U69,593 induced depolarizations (Fig. 4a). Given that the reversal potential for I_h is
150 depolarized compared to typical membrane potentials, the simplest possibility is that KOR
151 activation augments I_h conductance. Consistent with this, we found that U69,593 increased I_h
152 amplitude in a subset of neurons recorded in slices pretreated with CRF, and this response that
153 was not observed in control slices (Fig. 4b). CRF pretreatment did not impact other I_h properties
154 measured during U69,593 application (Extended Data Fig. 4).

155 Bruchas and colleagues reported that P38 MAPK contributes to some KOR mediated behavioral
156 changes following aversive stressors *in vivo*[33]. Here we tested for a contribution of p38 to this
157 KOR switch or KOR signaling. Incubating slices from control rats with the p38 blocker
158 SB203580 prior to CRF application prevented subsequent U69,593 induced depolarizations
159 (Fig. 4c). However, when slices were exposed to CRF prior to incubation in SB203580, U69,593
160 induced depolarizations persisted (Fig. 4a). We conclude that CRF receptor activation alters the
161 signaling of a subset of KORs in the VTA through a p38 dependent signaling pathway, but
162 KORs are not signaling through p38 directly to depolarize neurons.

Finally, we tested for a behavioral consequence of this change in KOR signaling. Decreases in dopamine neuron activity canonically encode punishment and aversion, and therefore intra-VTA KOR agonist induced aversion is widely thought to be due to inhibition of dopamine neurons. In the context of this model, a switch in KOR signaling in dopamine neurons from inhibitory to excitatory would be predicted to diminish conditioned place aversion (CPA) to intra-VTA KOR agonist microinjection. Since we found the switch in signaling sign to last between 3 and 5 days, we designed a paradigm where the animals received foot shock on days 1 and 6 in order to maintain stress-induced changes to KOR signaling. Pairings of either intra-VTA U69,593 (0.2 mM, 0.5 mL/side) or vehicle once per day were performed on non-stress days, for a total of four pairings per side (Fig. 5a), in order to minimize the formation of a direct association between the

foot shock stress and the place preference manipulation. Indeed, foot shock stress pretreatment eliminated the development of CPA to intra-VTA U69,593 (Fig. 5b, placements in Extended Data Fig. 5).

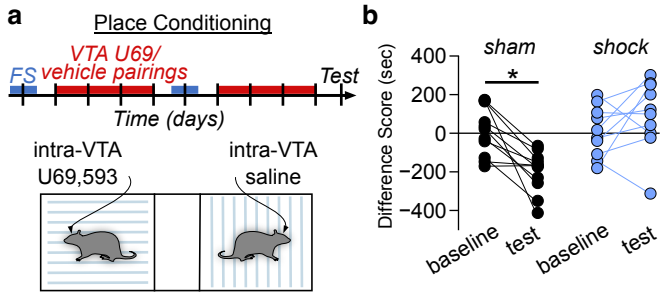

Figure 5. Foot shock stress eliminates intra-VTA KOR mediated aversion. *(a) Experiment timeline where rats were trained in a conditioned place preference paradigm, to intra-VTA U69,593 (0.2 mM, 0.5 mL/side) or vehicle. Rats were pretreated with sham handling or foot shock stress on non-pairing days. (b) Baseline vs post training test for place conditioning. Two way mixed measures ANOVA) Pairwise comparisons: Sham, baseline vs post test: 0.0004 Shock, baseline vs post test: 0.6 (Bonferroni corrected).*

Discussion

Together these data show that a single stressful event can dramatically change the signaling sign of a modulatory GPCR system. The change occurs in a specific neural circuit and can persist for days. This stress induced switch at KORs can be induced by the stress-associated CRF neuropeptide-GPCR system in the same brain region, and while the signaling is still G protein mediated, it appears that the key conductance involved is I_h, a switch from GIRK coupling.

The contributions of VTA dopamine neurons to the processing of aversive experiences encompass motivational and learning components and are circuit-specific[34]. *In vivo* electrophysiology studies show that while many midbrain putative and opto-tagged dopamine neurons decrease their firing when a predicted reward is omitted (i.e., an aversive outcome)[34,35], some putative and directly identified dopamine neurons increase their firing in response to an aversive sensory stimulus[36,37]. We previously demonstrated that in control rats, KOR activation inhibits VTA dopamine neurons that project to the mPFC and BLA, but not the NAc[18,19]. With microdialysis, we confirmed that *in vivo* VTA KOR activation decreases dopamine release in mPFC but not in the NAc[19]. Here we show a switch from inhibitory to excitatory signaling in a subpopulation of dmPFC-projecting VTA neurons after CRF exposure. This excitatory KOR effect may contribute to the reported stress induced activation of dmPFC-projecting VTA dopamine neurons[35,36]. The loss of intra-VTA KOR agonist induced CPA after the stress induced switch in KOR signaling also implicates the dopaminergic projection to dmPFC in value signaling. Consistent with this, MOR activation in the VTA causes an increase in dopamine release in the anterior cingulate cortex (ACC, included in the dmPFC in this study), and lesioning dopamine terminals there decreases the magnitude of intra-VTA MOR agonist induced conditioned place preference[15]. Also, genetic deletion of KOR from TH neurons and stress induced augmentation of cocaine CPP[37]. The transfer function of dopamine activity in the mPFC has been extensively studied, but a synthesized understanding of its contributions to mPFC processing of value remains somewhat elusive[38–40].

Here we discovered a convergence of two neuropeptide systems, with CRF changing the sign of the physiological response of KORs in a specific neural circuit. There are at least a dozen

192 possible sources of CRF to the VTA including the bed nucleus of the stria terminalis, dorsal
193 raphe, parabrachial nucleus, lateral dorsal tegmentum, and local VTA neurons[41,42] any of which
194 might be activated by aversive stressors. A subset of VTA neurons express CRF receptor 1
195 (CRF-R1) and the CRF binding protein, but not CRF receptor 2[43,44]. Blocking CRF-R1 in the
196 VTA decreases foot shock stress induced reinstatement of cocaine seeking[35]. Intra-VTA KOR
197 blockade[13] and intra-dmPFC dopamine antagonists also mitigate stress induced reinstatement
198 of cocaine seeking[35,45], a provocative parallel to the neuromodulatory circuit identified here.

199 We found that blocking I_h prevented KOR agonist induced depolarizations. Even though I_h is
200 generated by hyperpolarization activated, cyclic nucleotide-gated (HCN) channels[46,47] and thus
201 opioid receptors might interact with them though cAMP modulation, in the NRM KOR activation
202 in tissue from control rats augments I_h through a cAMP-independent signaling pathway that
203 involves intracellular release of Ca^{2+} [32]. In these neurons, cAMP activation causes a positive
204 shift in the voltage dependence of I_h, but does not change the maximum I_h amplitude. In the
205 VTA, the adenylyl cyclase activator forskolin causes a shift in the I_h $V_{1/2}$ to a more depolarized
206 potential[48]. The isoform HCN3, which is expressed in the vast majority of VTA dopamine
207 neurons and in many more VTA neurons than isoforms 1, 2 or 4[48], is relatively insensitive to
208 cAMP[46,49]. Here, KOR activation after CRF did not alter I_h $V_{1/2}$, consistent with a cAMP-
209 independent effect.

210 An increase in HCN channel function in the VTA has been implicated in behavioral changes
211 induced by aversive stressors. For instance, after social defeat stress in mice, I_h magnitude is
212 larger in VTA neurons of susceptible mice compared to those of control mice[50]. Blocking I_h in the
213 VTA[50,51] and systemically[52] reverse the social avoidance induced by social defeat. Our data
214 suggest that *in vivo* activity at KORs in the VTA after stress increases I_h function in dmPFC-
215 projecting dopamine neurons. Thus decreasing I_h function in the VTA may be one common
216 therapeutic target, be it through direct HCN blockade or KOR antagonism.

217 What are the *in vivo* consequences of this switch in KOR signaling? At the circuit level, this
218 switch means that the change in VTA dmPFC-projecting dopamine neuron firing will have an
219 opposite sign when an endogenous KOR ligand is released into the VTA. That is, the
220 peptidergic inputs to the VTA may have the same behavior-related firing patterns as before an
221 aversive stressor, but the impact on dmPFC dopamine release will be the inverse. In addition to
222 contributing to value encoding, dopamine function in the dmPFC also contributes to executive
223 function[16,17]. For instance, dopamine lesions in in the ACC impairs attentional set shifting[41] and
224 dopamine receptor antagonists delivered to the prelimbic cortex degrade decision making[42].
225 These and other studies suggest that ongoing or increases in dopamine release in the dmPFC
226 contribute to saliency processing, and support working memory[43], which are particularly
227 advantageous to engage following an aversive stressor. Following chronic stress that induces
228 anhedonia, activating mPFC-projecting VTA dopamine neurons reverses immobility and loss of
229 sucrose preference[44], and an increase in dopamine signaling in dmPFC also relieves ongoing
230 pain[45]. Provocatively, stress induced analgesia is also blocked by systemic administration of the
231 KOR selective antagonist norBNI[46], which in the context of our results would prevent an
232 increase in dopamine release in the dmPFC, although it is not yet known if dmPFC-projecting
233 VTA dopamine neurons contribute to this phenomenon. Together, these studies raise the
234 possibility that this switch in VTA KOR function is adaptive, with an optimal concentration of
235 dopamine in the mPFC facilitating learning. Learning about acutely aversive experiences, and
236 how to avoid them, is critical to survival.

237 **Methods**

238 **Animals.**

All experiments were performed in accordance with the guidelines of the National Institutes of Health Guide for the Care and Use of Laboratory Animals and the Institutional Animal Care and Use Committees (IACUC) at the University of California San Francisco. Male and female Sprague Dawley rats (p35 – p120 for electrophysiology; > 250g for behavior) were obtained from Inotiv or Charles River Laboratories. Rats were allowed access to food and water ad libitum and maintained on a reverse 12 h:12 h light/dark cycle. Rats were group housed except those with cannula implants.

Foot shock stress.
Operant chambers equipped with a foot shock grid were used for administering aversive stressors (physical boxes manufactured by Med. Associates with custom updated electronics controlled by microcontroller (Arduino)). Foot shock or sham sessions were 10 min, delivering 10, 0.8 mA intensity, 0.5 s duration shocks. Intervals between shocks were randomized (10 – 110 sec) in order to avoid predictability. Foot shock stress moderately elevated blood CORT, samples taken directly after foot shock session (Extended Data Fig. 6).

Electrophysiology.
Rats were deeply anesthetized with isoflurane, decapitated, and brains were quickly removed and cooled with ice-cold artificial cerebrospinal fluid (aCSF) consisting of (in mM): 119 NaCl, 2.5 KCl, 1.0 NaH_2PO_4, 26.2 $NaHCO_3$, 11 glucose, 1.3 $MgSO_4$, 2.5 $CaCl_2$, saturated with 95% O_2-5% CO_2, with a measured osmolarity 310–320 mOsm/L. Horizontal sections (150 µm) containing the VTA were cut with a Leica VT 1000 S or a Campden 7000smz-2 vibratome. Tissue containing the DiI injection sites was drop fixed in 4% formaldehyde to confirm targeting, with recordings in DiI labeled neurons made blind to injection target. Slices were incubated in oxygenated aCSF at 33 °C and allowed to recover for at least one hour. A single slice was placed in the recording chamber and continuously superfused with oxygenated aCSF (2 mL/min). Neurons were visualized with an upright microscope (Zeiss AxioExaminer.D1) equipped with infrared-differential interference contrast, Dodt optics, and fluorescent illumination. Whole-cell recordings were made at 34 °C using borosilicate glass microelectrodes (3–5 MΩ) filled with K-gluconate internal solution containing (in mM): 123 K-gluconate, 10 HEPES, 8 NaCl, 0.2 EGTA, 2 MgATP, 0.3 Na_3GTP, and 0.1% biocytin (pH 7.2 adjusted with KOH; 275 mOsm/L). Liquid junction potentials were not corrected. Input resistance was monitored throughout voltage clamp experiments with a −4 mV step every 30 s.
Signals were recorded using an Axopatch 1D (Molecular Devices, San Jose, CA) or IPA (Sutter Instruments, Novato, CA). Signals were filtered at 5 kHz and collected at 20 kHz using IGOR Pro (Wavemetrics) and custom data acquisition routines or collected at 10 kHz using SutterPatch software (Sutter Instruments).
Baseline hyperpolarization-activated cation currents (I_h) were recorded in each neuron by voltage clamping cells at -60 and stepping to -40, -50, -70, -80, -90, -100, -110, and -120 mV. Recordings were then made in current clamp mode (I = 0 pA). Changes in I_h properties were measured in voltage clamp, alternating between two step series (Extended Data Fig. 4) with one series commencing each 2.17 min.
After recordings, slices were drop fixed in 4% PFA for at least 2 h at 4 °C and processed for tyrosine hydroxylase (TH) immunocytochemistry and biocytin labeling. Recording were made from throughout the VTA.

Immunocytochemistry.
Slices were preblocked for 2 h at room temperature in PBS with 0.3% Tween20 and 5% normal goat serum, then incubated at 4°C with a rabbit anti-TH polyclonal antibody (1:400; EMD Millipore, RRID: AB_390204). Slices were then washed thoroughly in PBS with 0.3% Tween20

before being agitated overnight at 4°C with Cy5 anti-rabbit secondary antibody (1:1000; Jackson ImmunoResearch, RRID: AB_2534032) and FITC streptavidin (1:200; Jackson ImmunoResearch, AB_2337236). Tween20 was excluded in slices with DiI. Sections were rinsed and mounted on slides using VECTASHIELD® Antifade Mounting Media (Vector Laboratories) and visualized with an Axioskop FS2 Plus (Zeiss) with an Axiocam MRm (Zeiss) running Neurolucida (MBF Biosciences).

CORT ELISA.
Tail vein blood samples were collected immediately after foot shock or sham sessions from behavior animals. Trunk blood was collected at time of slice preparation for electrophysiology animals. Samples were centrifuged, then serum was frozen and stored at -80°C. ELISA kits were used as directed (DetectX Corticosterone Enzyme Immunoassay Kit (product # K014-H1); Arbor Assays).

Stereotaxic surgeries.
Tracer injections. Rats weighing 275–300 g were anesthetized with 3–5% isoflurane (Henry Schein) via inhalation and secured in a stereotaxic frame. Bilateral craniotomies were created with a dental drill above the injection site.

Tracer injections. Bilateral injections of DiI (7% in ethanol; Biotium, Hayward, CA) were made in the dmPFC (2.0 mm AP, ± 0.6 mm ML, -2.8 mm V), vmPFC (2.0 mm AP, ± 0.6 mm ML, -4.8 mm V), NAc (1.2 mm AP, ± 0.8 mm ML, -7.4 mm V), or basolateral amygdala (-3.3 mm AP, ± 5.0 mm ML, -8.4 mm V) using a Nanoject II (Drummond Scientific, Broomall, PA). 50 – 300 nL was injected in each hemisphere over ~5 min. The injector tip was left in place for at least 2 minutes after injection to decrease backflow and spread to tissue dorsal to the injection site. Recordings were made 7-8 days later.

Cannulation. For microinjections into the VTA, bilateral guide cannulae were implanted 1 mm above the VTA (−5.8 mm AP, ±0.5 mm ML,−7.2 mm DV). A dummy stylet was inserted to maintain patency of the cannulae. Cannulae were anchored with flat point screws and dental cement.

Analgesia and recovery. Rats were treated with subcutaneous Carprofen (5 mg/kg, Zoetis) and topical 2% lidocaine (Phoenix Pharmaceutical, Inc.) during the surgery for pain control. After surgery, animals had access to liquid Tylenol (~1:40) in their drinking water for 3–5 days or were administered Meloxicam (s.c. 2 mg/kg, Pivetal) once per day for two days. All DiI and cannulae placements were histologically verified postmortem.

Conditioned place preference.
Rats were allowed to recover for 1–2 weeks prior to behavioral testing. First, all rats were tested for bias in the conditioning boxes. The conditioning boxes (physical boxes purchased from Med. Associates, Georgia, VT, USA with custom updated electronics (Arduino; IR beam breaks (Adafruit)) and software have three divisions: two conditioning chambers (25 cm × 21 cm × 21 cm) with distinct visual (horizontal vs. vertical stripes) and textural (thick vs. thin mesh flooring) cues, separated by a smaller gray neutral chamber (12 cm × 21 cm × 21 cm). Animals were allowed up to three opportunities to show neutrality across the chambers during 20-min baseline sessions. Rats that displayed a consistent baseline preference (>65% of time spent in one chamber) were excluded from the study. Rats were pseudorandomly assigned to receive U69,593 in one of the conditioning chambers, and assignments were counter-balanced for each cohort.

The paradigm commenced with a foot shock or sham treatment as described above, completed in a different room from the conditioning chambers. Starting the next day, conditioning pairings (20 min) occurred once daily for 4 consecutive days alternating U69,593 (0.2 mM) and vehicle (0.5 mL/side). This 5 day series (including foot shock/sham) was repeated a second time for a total of 4 pairings for U69,593 and vehicle, each. Finally, on test day, rats were drug free and had access to all three chambers for 20 min. Difference score was defined as (Time spent in U69,593 paired chamber)−(Time spent in vehicle paired chamber).

Microinjections. Rats were lightly restrained in a cloth wrap for intracranial microinjections. A bilateral 33 G microinjector (PlasticsOne) that extended 1 mm ventrally beyond the guide cannula was inserted to deliver drug. Hamilton syringes were driven by a dual syringe pump to deliver the injection volume over 2 min. Injectors were left in place for 1 min after injection.

Brain removal and histochemistry. To check cannulae placements, rats were deeply anesthetized with an intraperitoneal injection of Euthasol (0.1 mg/kg, Virbac Animal Health) after 0.3 µL of Chicago Sky Blue (in 2% PBS) was injected through the cannulae to mark injection locations. After becoming unresponsive to noxious stimuli, the rats were transcardially perfused with 400 mL of saline, followed by 400 mL of 4% paraformaldehyde (PFA) in 0.1 M phosphate buffer. The brains were extracted and immersion-fixed in PFA for 2 h at room temperature (RT), washed two times with PBS to remove excess PFA, and stored in 1X PBS at 4°C.
Perfused brains and drop fixed DiI containing tissue were sectioned (50 µm) using a vibratome (Leica VT 1000S). Alternating slices were Nissl stained. Sections were mounted on slides using VECTASHIELD® mounting medium (Vector Laboratories). Microinjection locations for rats included in the behavior study are summarized in Extended Data Fig. 5.

Data analysis.
The magnitude of U69,593 induced changes in V_m were quantified by comparing the mean values over the last 4 min of U69,593 application to the 4 minutes of baseline just prior to starting the drug application. Responses were tested for significance by statistically comparing 30 sec bins during these two time periods (unpaired Student's t-test). I_h magnitude was measured as the difference between the initial capacitive response to a voltage step from −60 to −120 mV and the final current during the same step. Reported baseline Ri and firing rate are the average measurements over the first 2 min of I_{clamp} recording. For AP duration measurements, at least 8 waveforms were averaged together and duration was calculated from threshold on the ascending phase to recrossing threshold on the falling phase. Threshold was identified as the first datapoint where the derivative of the waveform exceeds 10 V/s. For evaluation of KOR agonist induced changes in I_h properties, see measurements described in Extended Data Fig. 4.

Population statistics were performed in R. Where datasets failed tests of normality or homogeneity of variance, non-parametric permutation analyses (https://github.com/eb-margolis-neuroscience-lab/R-general-Margolislab/tree/main) were used to test for statistical significance. For behavior data, mixed measures two-way ANOVA was used with Bonferroni correction for multiple comparisons.

Acknowledgements
I thank Joseph R. Driscoll, Thomas J. Cirino, Peter Fong, Aashka Popat, Ben J. Ngu, Benjamin Snyder, Kasra Mansorian, and Madelyn Moulton for technical assistance. This work was supported by National Institutes of Health grants R01DA030529, R01DA042025 and R01DA008863, and funds from the State of California for medical research on alcohol and substance use.

Figure Captions

Figure 1. Following a single foot shock session, a subset of VTA neurons depolarize in response to KOR activation. (a) Rats experienced a single intermittent foot shock session (10 min) prior to *ex vivo* whole cell recordings. (b) Example recording from a VTA neuron (biocytin fill: red) that was confirmed as dopaminergic with TH immunocytochemistry (green), scale bar 10 μm. In whole cell current clamp configuration (I = 0 pA) bath application of the KOR agonist U69,592 (1 μM) caused a depolarization. Inset: I_h measured in voltage clamp, scale bars 200 pA and 200 ms. (c) Mean time course of responses in neurons that were significantly depolarized by U69,593. (d) Summarized data, each circle is a neuron, from same day sham shock, same day shock, 3 days after shock and 5 days after shock treated rats. Circles and triangles indicate VTA neurons from male and female rats, respectively. Permutation analysis comparing means of U69,593 responses in sham vs shock, p = 0.02 (Table 1) (e) Summarized U69,593 responses in VTA neurons from naïve rats, and from naïve rats where U69,593 responses were measured in $BaCl_2$ (100 μM). Statistical comparison performed was permutation analysis comparing variances (SDs; $ indicates p<0.05), p = 0.04. (f) Summarized responses to the dopamine D2 receptor agonist quinpirole (1 μM) in VTA neurons from naïve, sham, and foot shocked rats. One way ANOVA sham vs shock, p = 0.9.

Figure 2. *ex vivo* exposure to CRF can switch KOR signaling from inhibitory to excitatory. (a) Summarized data, each circle is a neuron. Slices were incubated for 5 min with CRF (200 nM), CRF was washed out for at least 5 min, then U69,593 (1 μM) was bath applied for 5 min. Statistical comparison to U69,593 responses in VTA neurons from naïve rats (Fig. 1e left), Permutation analysis of means, p = 0.00004. (b) Left, U69,593 (1 μM) was applied once, washed out, then reapplied (paired t-test p = 1.0). Right, U69,593 (1 μM) was applied once, washed out, CRF was washed on (5 min, 200 nM), washed out, then U69,593 was reapplied (paired t-test p = 0.08). (c) Data from (b) graphed as magnitude of response to first U69,593 application to second application.

Figure 3. CRF switches KOR signaling in a subpopulation of dmPFC-projecting VTA neurons. U69,593 responses were recorded in retrogradely labeled neurons after slices were incubated in CRF (5 min, 200 nM). Kruskal-Wallis rank sum test p = 0.006, pairwise comparisons listed in Table 1.

Figure 4. KOR mediated depolarizations require I_h. (a) Signaling mechanism(s) that contribute to U69,593 (1 μM) induced depolarizations were investigated after exposing slices *ex vivo* to CRF (5 min, 200 nM). TTX (500 nM), DNQX (10 μM), and gabazine (20 μM) blocked synaptic transmission; intracellular GDP-β-s (500 μM) blocked intracellular G protein signaling; ZD7288 (10 μM) blocked HCN channels (I_h); $BaCl_2$ (100 μM) blocked K^+ channels; $CdCl_2$ (100 μM) blocked Ca^{2+} channels; replacement of Na^+ with NMDG (151 mM, replacing NaCl) in aCSF blocked Na^+ leak current; SB203580 (10 μM) blocked p38/MAPK signaling. (b) I_h magnitude was measured during U69,593 (1 μM) application in voltage clamp, stepping from -60 mV to -120 mV, in control slices or slices pretreated with CRF (5 min, 200 nM). (c) p38/MAPK was blocked with SB203580 application during both CRF and U69,593 application.

Figure 5. Foot shock stress eliminates intra-VTA KOR mediated aversion. (a) Experiment timeline where rats were trained in a conditioned place preference paradigm, to intra-VTA U69,593 (0.2 mM, 0.5 mL/side) or vehicle. Rats were pretreated with sham handling or foot shock stress on non-pairing days. (b) Baseline vs post training test for place conditioning. Two way mixed measures ANOVA) Pairwise comparisons: Sham, baseline vs post test: 0.0004 Shock, baseline vs post test: 0.6 (Bonferroni corrected).

Extended Data Figure 1. (a) Summary of responses to U69,593 in neurons identified at TH(+) with immunocytochemistry. These are a subset of the data in Fig. 1d. (b) Locations of VTA neurons recorded from same day foot shock stress rats. Color indicates change in Vm in response to U69,593.

Extended Data Figure 2. Physiological properties recorded in VTA neurons from foot shock (same day) or sham rats. Quantifications of data collected during the first 150 s immediately after whole cell access is achieved. (a) Ri, (b) AP duration, (c) AP threshold, (d) AP peak, (e) I_h magnitude (f) spontaneous firing rate. $^{**}p < 0.01$

Extended Data Figure 3. Foot shock rat data from Supplementary Figure 2, sorted by the type of response to U69,593. (a) Ri, (b) AP duration, (c) AP threshold, (d) AP peak, (e) I_h magnitude $^{*}p < 0.05$

Extended Data Figure 4. I_h measurements. (a) top, schematic of V step commands from V=-40 mV to quantify $V_{1/2}$ and activation τ. Bottom, example response. (b) top, schematic of V step commands from V = -40 mV to quantify reversal V. Bottom, example response from the same neuron as in (a). (c) Example single exponential fit to data in (a). (d) Schematic of experiment design. Step series shown in (a) and (b) were applied to each neuron for a "baseline" measurement and again during U69,593 application. (e) Difference between $V_{1/2}$ measured at baseline and in U69,593. Grey is no pretreatment, Orange is CRF pretreatment. (f) Difference between $V_{reverse}$ measured at baseline and in U69,593. Grey is no pretreatment, Orange is CRF pretreatment. (g) I_h activation τ at baseline vs in U69,593. Grey is no pretreatment, Orange is CRF pretreatment.

Extended Data Figure 5. Microinjection sites for intra-VTA place conditioning experiments in Figure 5.

Extended Data Figure 6. CORT measured (ELISA) from trunk blood samples collected from same day foot shock and sham animals during brain slice preparation. * p = 0.05

References

1. Varlinskaya, E. I., Spear, L. P. & Diaz, M. R. Stress alters social behavior and sensitivity to pharmacological activation of kappa opioid receptors in an age-specific manner in Sprague Dawley rats. *Neurobiol. Stress* **9**, 124–132 (2018).
2. McLaughlin, J. P., Li, S., Valdez, J., Chavkin, T. A. & Chavkin, C. Social defeat stress-induced behavioral responses are mediated by the endogenous kappa opioid system. *Neuropsychopharmacology* **31**, 1241–8 (2006).

474 3. Massaly, N. *et al.* Pain-Induced Negative Affect Is Mediated via Recruitment of The
475 Nucleus Accumbens Kappa Opioid System. *Neuron* (2019)
476 doi:10.1016/j.neuron.2019.02.029.
477 4. Groblewski, P. A., Zietz, C., Willuhn, I., Phillips, P. E. M. & Chavkin, C. Repeated stress
478 exposure causes strain-dependent shifts in the behavioral economics of cocaine in rats.
479 *Addict. Biol.* **20**, 297–301 (2015).
480 5. Carlezon Jr., W. A. & Krystal, A. D. Kappa-Opioid Antagonists for Psychiatric Disorders:
481 From Bench to Clinical Trials. *Depress. Anxiety* **33**, 895–906 (2016).
482 6. Reeves, K. C., Shah, N., Muñoz, B. & Atwood, B. K. Opioid Receptor-Mediated Regulation
483 of Neurotransmission in the Brain. *Front. Mol. Neurosci.* **15**, 919773 (2022).
484 7. Ji, M. *et al.* Dynorphin promotes stress-induced depressive behaviors by inhibiting
485 ventral pallidal neurons in rats. *Acta Physiol.* **236**, (2022).
486 8. Lemos, J. C. *et al.* Repeated stress dysregulates κ-opioid receptor signaling in the dorsal
487 raphe through a p38α MAPK-dependent mechanism. *J. Neurosci. Off. J. Soc. Neurosci.* **32**,
488 12325–12336 (2012).
489 9. Pan, Z. Z., Tershner, S. A. & Fields, H. L. Cellular mechanism for anti-analgesic action of
490 agonists of the kappa-opioid receptor. *Nature* **389**, 382–385 (1997).
491 10. Margolis, E. B., Hjelmstad, G. O., Bonci, A. & Fields, H. L. Kappa-opioid agonists directly
492 inhibit midbrain dopaminergic neurons. *J Neurosci* **23**, 9981–6 (2003).
493 11. Bals-Kubik, R., Ableitner, A., Herz, A. & Shippenberg, T. S. Neuroanatomical sites
494 mediating the motivational effects of opioids as mapped by the conditioned place
495 preference paradigm in rats. *J Pharmacol Exp Ther* **264**, 489–95 (1993).

496 12. Ehrich, J. M. *et al.* Kappa Opioid Receptor-Induced Aversion Requires p38 MAPK
497 Activation in VTA Dopamine Neurons. *J Neurosci* **35**, 12917–31 (2015).
498 13. Graziane, N. M., Polter, A. M., Briand, L. A., Pierce, R. C. & Kauer, J. A. Kappa opioid
499 receptors regulate stress-induced cocaine seeking and synaptic plasticity. *Neuron* **77**,
500 942–954 (2013).
501 14. Vijayraghavan, S., Major, A. J. & Everling, S. Neuromodulation of Prefrontal Cortex in
502 Non-Human Primates by Dopaminergic Receptors during Rule-Guided Flexible
503 Behavior and Cognitive Control. *Front. Neural Circuits* **11**, 91 (2017).
504 15. Narita, M. *et al.* Implication of dopaminergic projection from the ventral tegmental area
505 to the anterior cingulate cortex in μ-opioid-induced place preference. *Addict. Biol.* **15**,
506 434–447 (2010).
507 16. Tichelaar, J. G., Sayalı, C., Helmich, R. C. & Cools, R. Impulse control disorder in
508 Parkinson's disease is associated with abnormal frontal value signalling. *Brain J. Neurol.*
509 **146**, 3676–3689 (2023).
510 17. Cools, R., Froböse, M., Aarts, E. & Hofmans, L. Dopamine and the motivation of cognitive
511 control. *Handb. Clin. Neurol.* **163**, 123–143 (2019).
512 18. Margolis, E. B., Mitchell, J. M., Ishikawa, J., Hjelmstad, G. O. & Fields, H. L. Midbrain
513 dopamine neurons: projection target determines action potential duration and
514 dopamine D(2) receptor inhibition. *J Neurosci* **28**, 8908–13 (2008).
515 19. Margolis, E. B. *et al.* Kappa opioids selectively control dopaminergic neurons projecting
516 to the prefrontal cortex. *Proc Natl Acad Sci U A* **103**, 2938–42 (2006).

517 20. Seutin, V., Johnson, S. W. & North, R. A. Effect of dopamine and baclofen on N-methyl-D-
518 aspartate-induced burst firing in rat ventral tegmental neurons. *Neuroscience* **58**, 201–
519 206 (1994).
520 21. Land, B. B. *et al.* The dysphoric component of stress is encoded by activation of the
521 dynorphin kappa-opioid system. *J Neurosci* **28**, 407–14 (2008).
522 22. Bruchas, M. R., Land, B. B., Lemos, J. C. & Chavkin, C. CRF1-R activation of the
523 dynorphin/kappa opioid system in the mouse basolateral amygdala mediates anxiety-
524 like behavior. *PloS One* **4**, e8528 (2009).
525 23. Van't Veer, A., Yano, J. M., Carroll, F. I., Cohen, B. M. & Carlezon, W. A. Corticotropin-
526 releasing factor (CRF)-induced disruption of attention in rats is blocked by the κ-opioid
527 receptor antagonist JDTic. *Neuropsychopharmacol. Off. Publ. Am. Coll.*
528 *Neuropsychopharmacol.* **37**, 2809–2816 (2012).
529 24. Wang, B. *et al.* Cocaine experience establishes control of midbrain glutamate and
530 dopamine by corticotropin-releasing factor: a role in stress-induced relapse to drug
531 seeking. *J Neurosci* **25**, 5389–96 (2005).
532 25. Xia, Y.-F., Margolis, E. B. & Hjelmstad, G. O. Substance P inhibits GABAB receptor
533 signalling in the ventral tegmental area. *J. Physiol.* **588**, 1541–1549 (2010).
534 26. Margolis, E. B., Hjelmstad, G. O., Fujita, W. & Fields, H. L. Direct bidirectional μ-opioid
535 control of midbrain dopamine neurons. *J Neurosci* **34**, 14707–16 (2014).
536 27. Margolis, E. B., Fujita, W., Devi, L. A. & Fields, H. L. Two delta opioid receptor subtypes
537 are functional in single ventral tegmental area neurons, and can interact with the mu
538 opioid receptor. *Neuropharmacology* **123**, 420–432 (2017).

539 28. Cobb-Lewis, D. E., Sansalone, L. & Khaliq, Z. M. Contributions of the Sodium Leak
540 Channel NALCN to Pacemaking of Medial Ventral Tegmental Area and Substantia Nigra
541 Dopaminergic Neurons. *J. Neurosci. Off. J. Soc. Neurosci.* **43**, 6841–6853 (2023).
542 29. Khaliq, Z. M. & Bean, B. P. Pacemaking in dopaminergic ventral tegmental area neurons:
543 depolarizing drive from background and voltage-dependent sodium conductances. *J.*
544 *Neurosci. Off. J. Soc. Neurosci.* **30**, 7401–7413 (2010).
545 30. Philippart, F. & Khaliq, Z. M. Gi/o protein-coupled receptors in dopamine neurons
546 inhibit the sodium leak channel NALCN. *eLife* **7**, e40984 (2018).
547 31. Ingram, S. L. & Williams, J. T. Opioid inhibition of Ih via adenylyl cyclase. *Neuron* **13**,
548 179–186 (1994).
549 32. Pan, Z. Z. κ-Opioid receptor-mediated enhancement of the hyperpolarization-activated
550 current (Ih) through mobilization of intracellular calcium in rat nucleus raphe magnus.
551 *J. Physiol.* **548**, 765–775 (2003).
552 33. Bruchas, M. R. *et al.* Stress-induced p38 mitogen-activated protein kinase activation
553 mediates kappa-opioid-dependent dysphoria. *J Neurosci* **27**, 11614–23 (2007).
554 34. Morales, M. & Margolis, E. B. Ventral tegmental area: cellular heterogeneity,
555 connectivity and behaviour. *Nat Rev Neurosci* (2017) doi:10.1038/nrn.2016.165.
556 35. Vranjkovic, O. *et al.* Enhanced CRFR1-Dependent Regulation of a Ventral Tegmental
557 Area to Prelimbic Cortex Projection Establishes Susceptibility to Stress-Induced
558 Cocaine Seeking. *J. Neurosci. Off. J. Soc. Neurosci.* **38**, 10657–10671 (2018).
559 36. Deutch, A. Y. *et al.* Stress selectively increases fos protein in dopamine neurons
560 innervating the prefrontal cortex. *Cereb. Cortex N. Y. N 1991* **1**, 273–292 (1991).

561 37. Abraham, A. D., Casello, S. M., Land, B. B. & Chavkin, C. Optogenetic stimulation of
562 dynorphinergic neurons within the dorsal raphe activate kappa opioid receptors in the
563 ventral tegmental area and ablation of dorsal raphe prodynorphin or kappa receptors
564 in dopamine neurons blocks stress potentiation of cocaine reward. *Addict. Neurosci.* **1**,
565 100005 (2022).
566 38. Sheynikhovich, D., Otani, S., Bai, J. & Arleo, A. Long-term memory, synaptic plasticity and
567 dopamine in rodent medial prefrontal cortex: Role in executive functions. *Front. Behav.*
568 *Neurosci.* **16**, 1068271 (2023).
569 39. Durstewitz, D. & Seamans, J. K. The dual-state theory of prefrontal cortex dopamine
570 function with relevance to catechol-o-methyltransferase genotypes and schizophrenia.
571 *Biol. Psychiatry* **64**, 739–749 (2008).
572 40. Robinson, S. E. & Sohal, V. S. Dopamine D2 Receptors Modulate Pyramidal Neurons in
573 Mouse Medial Prefrontal Cortex through a Stimulatory G-Protein Pathway. *J. Neurosci.*
574 *Off. J. Soc. Neurosci.* **37**, 10063–10073 (2017).
575 41. Soden, M. E. *et al.* Distinct Encoding of Reward and Aversion by Peptidergic BNST
576 Inputs to the VTA. *Front. Neural Circuits* **16**, 918839 (2022).
577 42. Grieder, T. E. *et al.* VTA CRF neurons mediate the aversive effects of nicotine
578 withdrawal and promote intake escalation. *Nat. Neurosci.* **17**, 1751–1758 (2014).
579 43. Van Pett, K. *et al.* Distribution of mRNAs encoding CRF receptors in brain and pituitary
580 of rat and mouse. *J. Comp. Neurol.* **428**, 191–212 (2000).
581 44. Wang, H.-L. & Morales, M. Corticotropin-releasing factor binding protein within the
582 ventral tegmental area is expressed in a subset of dopaminergic neurons. *J. Comp.*
583 *Neurol.* **509**, 302–318 (2008).

584 45. McFarland, K. & Kalivas, P. W. The circuitry mediating cocaine-induced reinstatement of
585 drug-seeking behavior. *J. Neurosci. Off. J. Soc. Neurosci.* **21**, 8655–8663 (2001).
586 46. Combe, C. L. & Gasparini, S. Ih from synapses to networks: HCN channel functions and
587 modulation in neurons. *Prog. Biophys. Mol. Biol.* **166**, 119–132 (2021).
588 47. Monteggia, L. M., Eisch, A. J., Tang, M. D., Kaczmarek, L. K. & Nestler, E. J. Cloning and
589 localization of the hyperpolarization-activated cyclic nucleotide-gated channel family in
590 rat brain. *Mol. Brain Res.* **81**, 129–139 (2000).
591 48. Mu, L. *et al.* cAMP-mediated upregulation of HCN channels in VTA dopamine neurons
592 promotes cocaine reinforcement. *Mol. Psychiatry* **28**, 3930–3942 (2023).
593 49. Mistrík, P. *et al.* The Murine HCN3 Gene Encodes a Hyperpolarization-activated Cation
594 Channel with Slow Kinetics and Unique Response to Cyclic Nucleotides. *J. Biol. Chem.*
595 **280**, 27056–27061 (2005).
596 50. Cao, J.-L. *et al.* Mesolimbic dopamine neurons in the brain reward circuit mediate
597 susceptibility to social defeat and antidepressant action. *J. Neurosci. Off. J. Soc. Neurosci.*
598 **30**, 16453–16458 (2010).
599 51. Cai, M. *et al.* HCN channel inhibitor induces ketamine-like rapid and sustained
600 antidepressant effects in chronic social defeat stress model. *Neurobiol. Stress* **26**,
601 100565 (2023).
602 52. Teichman, E. M. *et al.* Design and validation of novel brain-penetrant HCN channel
603 inhibitors to ameliorate social stress-induced susceptible phenotype. *Mol. Psychiatry*
604 (2025) doi:10.1038/s41380-025-02972-8.
605
606

Table 1 – Assumption testing and statistical comparisons for summary data						
Experiment	**Figure**	**# Neurons; # Outliers; # Extreme outliers**	**Shapiro-Wilk test of Normality Statistic; p val**	**Test for Homogeneity of Variances Statistic; p val (Test used)**	**Parametric test Statistic; p val (Test used)**	**Non-parametric test Statistic and/or p val (Test used)**
U69,593 response (mV), acute stress vs sham	1d	67; 3; 0	0.9; 0.00008	7.5; 0.008 (Levene's)	n/a	0.02 (Permutation, mean)
U69,593 response in $BaCl_2$ vs acute stress	1d,e	49; 4; 0	0.9; 0.0007	3.0; 0.09 (Levene's)	n/a	0.04 (Permutation, SD)
Quinpirole response (mV), acute stress vs sham	1f	27; 2; 1	1.0; 0.6	1.4; 0.2 (Levene's)	0.02; 0.9 (one way ANOVA)	n/a
U69.593 response naïve vs after CRF	1e, 2a	78; 2; 0	1.0; 0.02	0.9; 0.4 (Levene's)	n/a	0.00004
U69,593, first application vs second application	2b, left	6; 0; 0	0.9; 0.6	0.02; 0.9	0.0003; 1.0 (paired t-test)	
U69,593 responses pre- vs post- CRF	2b, right	10; 0; 0	1.0; 0.7	2.0; 0.2	-2.0; 0.08 (paired t-test)	
U69,593, first application vs second application	2c	6; 0; 0			5.1; 0.007 (Pearson's product moment correlation, coeff = 0.9)	
U69,593 responses pre- vs post- CRF, in neurons with a post-CRF U69,593 induced depolarization	Subset in 2c	5			-3.7; 0.03 (Pearson's product moment correlation, coeff = -0.9)	
U69,593 responses differ by projection target	3	48; 6; 3	0.8; 0.0000001	1.4; 0.3	n/a	12.4; 0.006 (Kruskal-Wallis rank sum test) Pairwise comparisons (p adjustment method BH): dmPFC-BLA: 0.05 dmPFC-NAc: 0.05 dmPFC-vmPFC: 0.03 BLA-NAc: 0.4 BLA-vmPFC: 0.4 NAc-vmPFC: 0.2
U69,593 after CRF vs after CRF with GDP-β-s	4a	34; 1; 0	0.9; 0.007	4.4; 0.05	n/a	0.01 (Permutation, SD)
U69,593 after CRF vs after CRF with ZD7288	4a	39; 2; 1	0.9; 0.06	2.5; 0.1	0.7; 0.4 (one way ANOVA)	
U69,593 after CRF vs after CRF with TTX, DNQX, gabazine	4a	47; 4; 0	0.9; 0.005	1.2; 0.3	n/a	0.3 (Permutation, mean)
U69,593 after CRF vs after CRF with $BaCl_2$	4a	38; 1; 0	0.9; 0.01	2.5; 0.1	n/a	0.5 (Permutation, mean)
U69,593 after CRF vs after CRF with $CdCl_2$	4a	33; 1; 0	0.9; 0.007	0.01; 0.9	n/a	0.6 (Permutation, mean)
U69,593 after CRF vs after CRF with NMDG	4a	31; 1; 0	0.9; 0.01	1.1; 0.3	n/a	0.2 (Permutation, mean)
U69,593 after CRF vs after CRF with SB203580 (only during U69,593)	4a	36; 1; 0	0.9; 0.00008	7.5; 0.008	n/a	0.4 (Permutation, mean)
I_h magnitude after U69,593, with vs without CRF pretreatment	4b	18; 2; 0	0.9; 0.02	1.7; 0.2	n/a	0.3 (Permutation, mean)
U69,593 after CRF vs after CRF with SB203580 (applied	4a,c	34; 2; 0	1.0; 0.2	0.0007; 1.0	3.8; 0.06	

during CRF and U69,593)						
Intra-VTA U69,593 place conditioning, sham- vs shock-treated rats	5b	20 rats; 0; 0	Base-sham: 1.0; 0.8 Base-shock: 0.9; 0.6 Sham-test: 0.9; 0.5 Shock-test: 0.9; 0.4	Sham: 0.9; 0.4 Shock: 3.5; 0.08	Pretreatment-U69,593 interaction: 9.0; 0.008 (Two way mixed measures ANOVA) Pairwise comparisons: Sham, Base vs test: 0.0004 Shock, Base vs test: 0.6 (Bonferroni corrected)	
Baseline Ri in neurons from stress vs sham animals	Supp 2	139; 0; 0	1.0; 0.01	0.5; 0.5		0.2 (Permutation, mean)
Spontaneous AP duration in neurons from stress vs sham animals	Supp 2	81; 1; 0	0.9; 0.00002	0.9; 0.3		0.8 (Permutation, mean)
Spontaneous AP threshold in neurons from stress vs sham animals	Supp 2	81; 0; 0	1.0; 0.8	0.9; 0.3	9.5; 0.003 (one way ANOVA)	
Spontaneous AP peak in neurons from stress vs sham animals	Supp 2	81; 1; 0	1.0; 0.09	1.5; 0.2	0.2; 0.7 (one way ANOVA)	
I_h magnitude in neurons from stress vs sham animals	Supp 2	129; 17; 10	0.6; <0.000001	0.5; 0.5		0.4 (Permutation, mean)
Baseline spontaneous firing rate in neurons from stress vs sham animals	Supp 2	60; 5; 3	0.8; <0.000001	0.4; 0.5		0.3 (Permutation, mean)
Proportion of spontaneously active neurons from stress vs sham animals						0.9 (two tailed Fisher exact test)
Baseline Ri in neurons from stress animals grouped by U69,593 response type	Supp 3	46; 0; 0	1.0; 0.4	0.2; 0.8	3.2; 0.04 (one way ANOVA) Pairwise comparisons: Inhib-excit: 0.04 Inhib-no resp: 0.2 Excit-no resp: 0.9	
AP duration in neurons from stress animals grouped by U69,593 response type	Supp 3	27; 0; 0	0.9; 0.1	4.4; 0.02		3.1; 0.2 (Kruskal-Wallis rank sum test)
AP threshold in neurons from stress animals grouped by U69,593 response type	Supp 3	27; 0; 0	1.0; 0.4	1.5; 0.2	0.3; 0.7 (one way ANOVA)	
AP peak in neurons from stress animals grouped by U69,593 response type	Supp 3	27; 1; 0	0.9; 0.1	0.6; 0.5	0.8 (one way ANOVA)	

CORT from recording animals, foot shock vs sham	Supp 6	16 rats; 1; 0	0.9; 0.2	0.09; 0.8	0.05 (one way ANOVA)	

Extended Data Figure 1

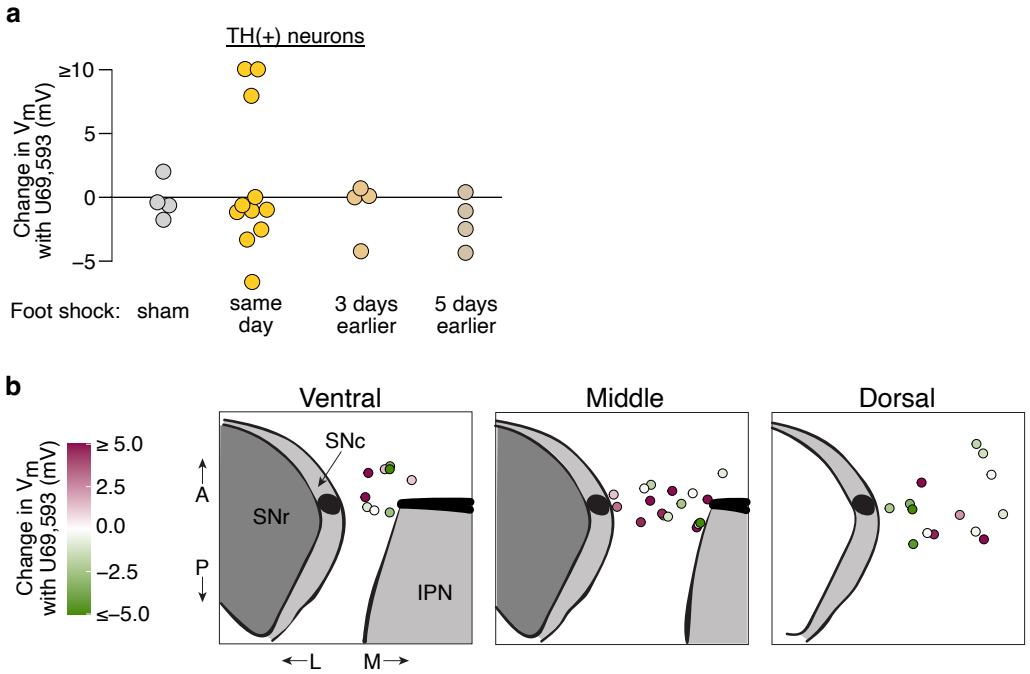

Extended Data Figure 2

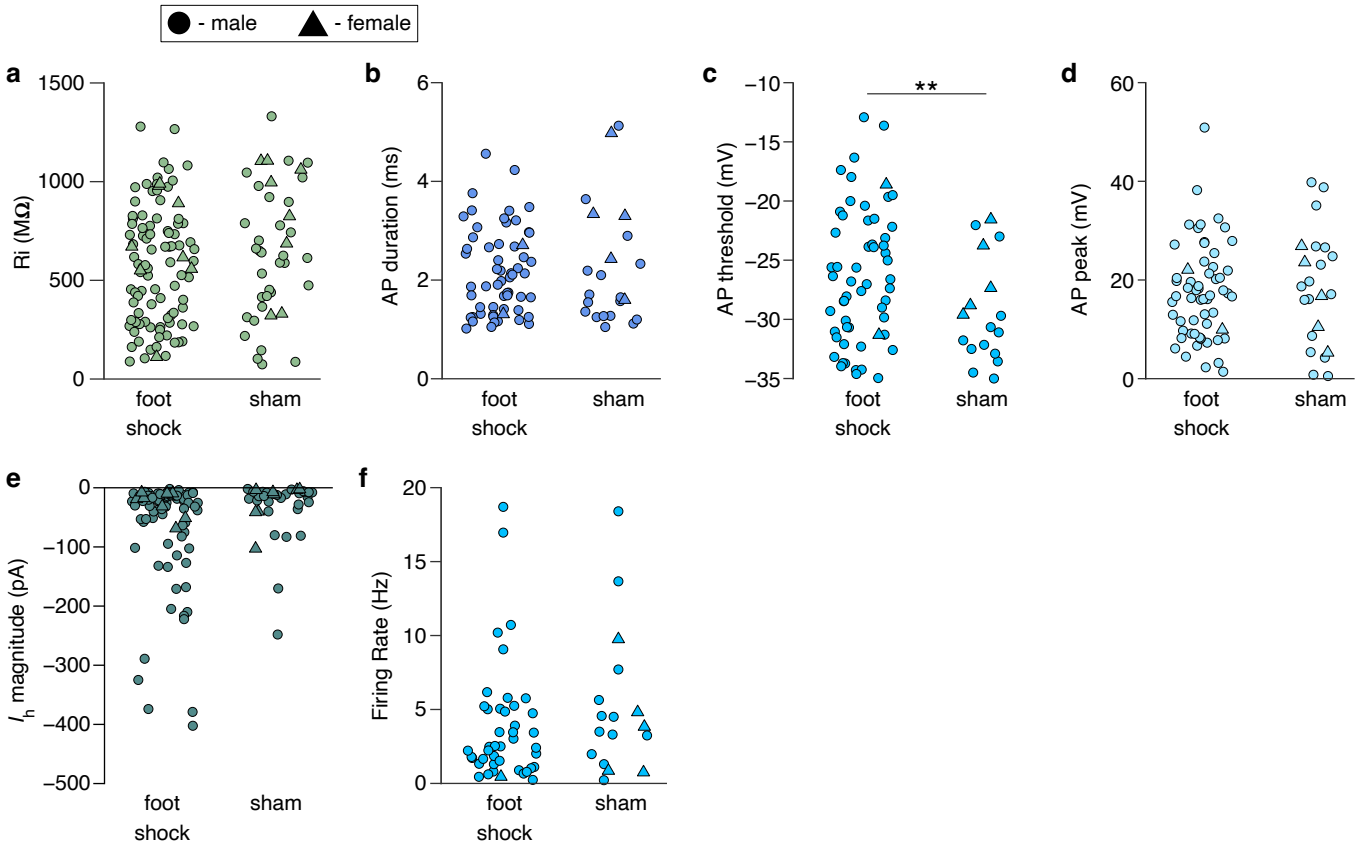

Extended Data Figure 3

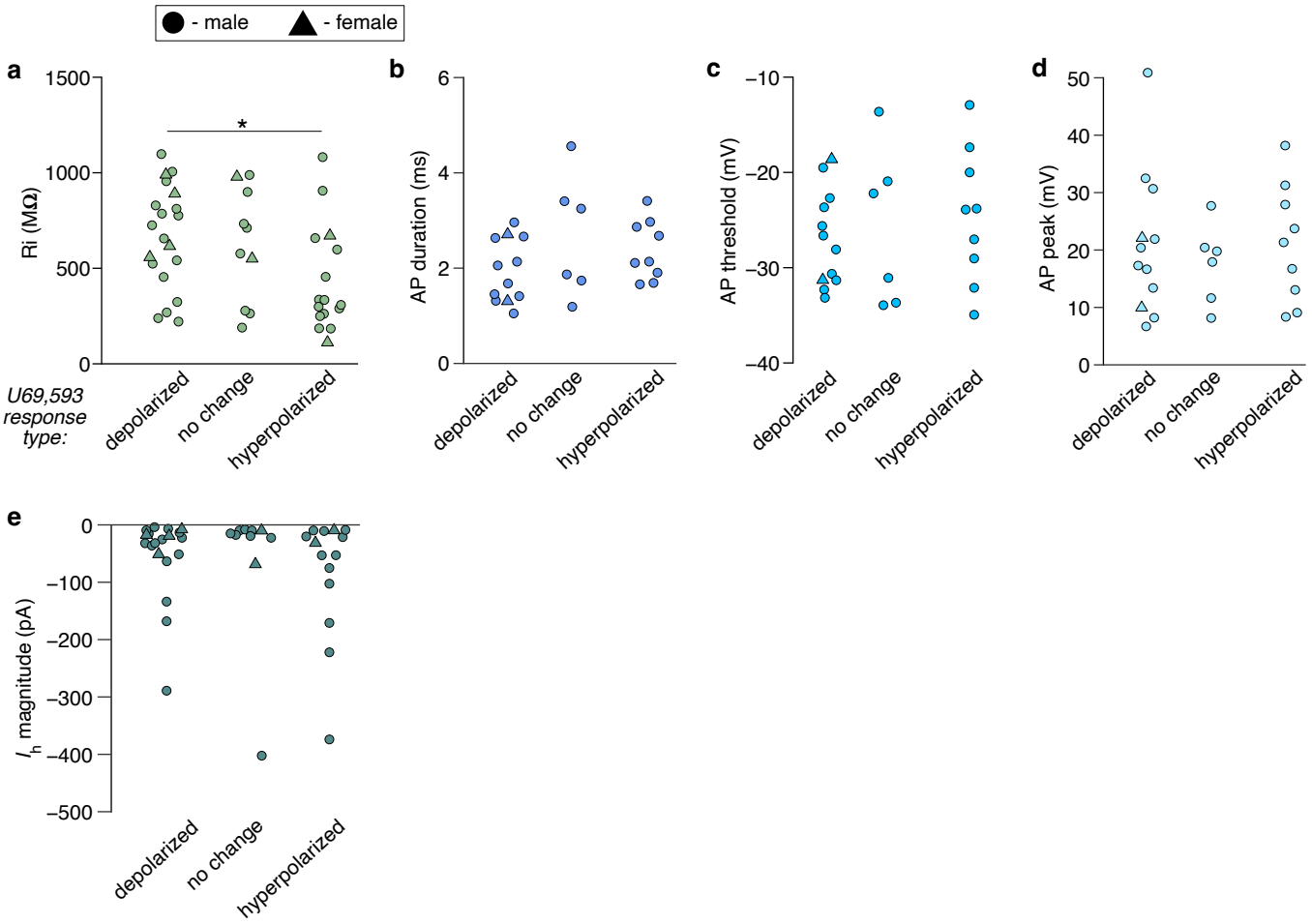

Extended Data Figure 4

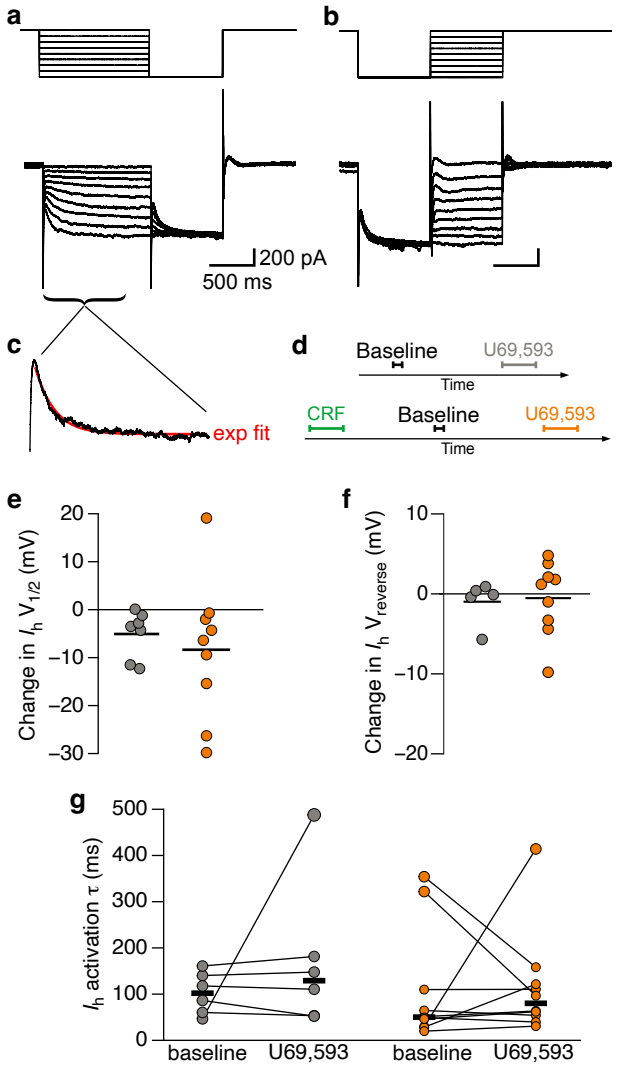

Extended Data Figure 5

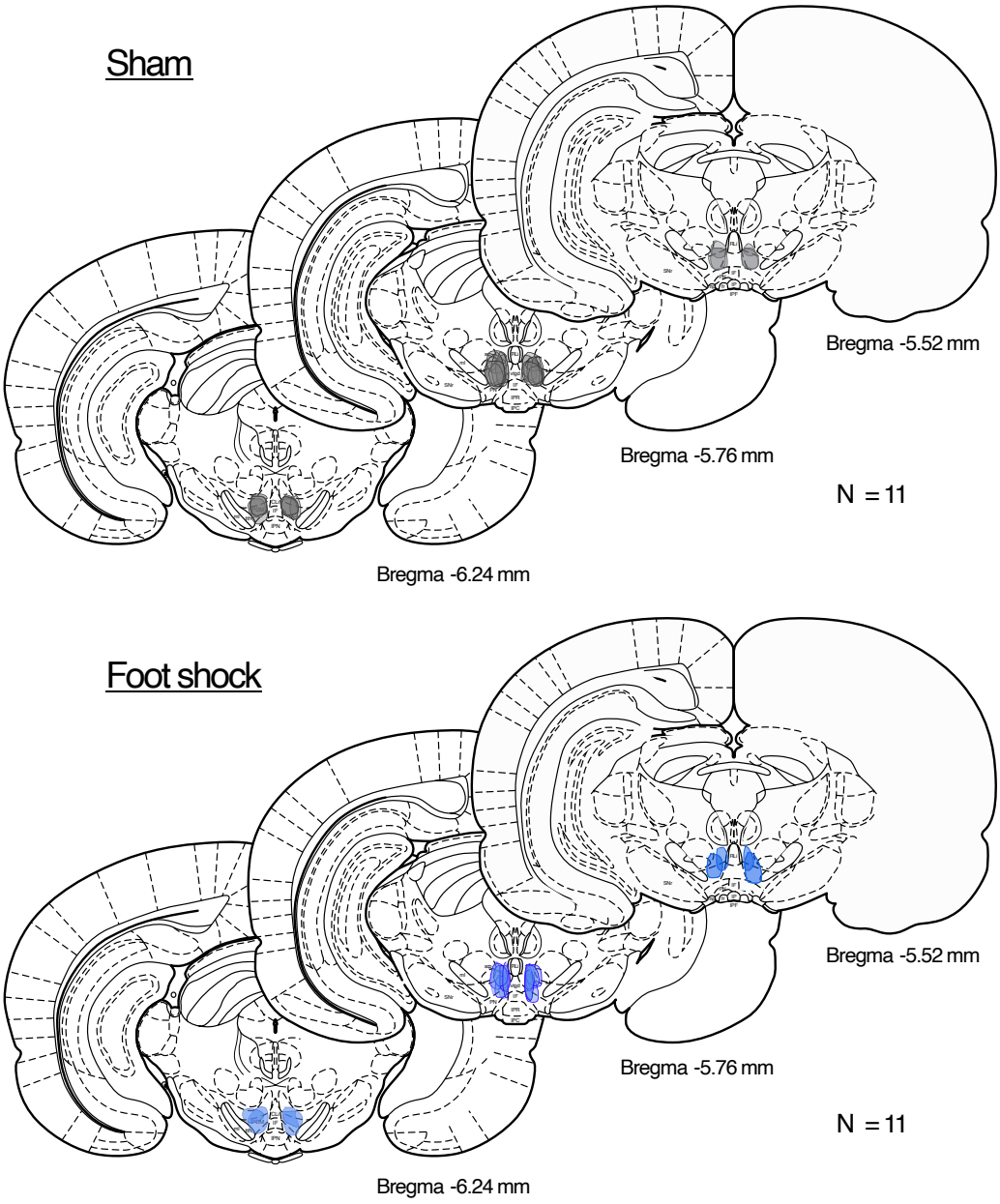
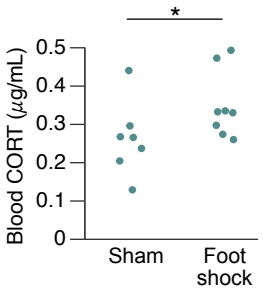
Extended Data Figure 6